British Journal of Pharmacology (2008) 153, 1513–1527
 0007–1188/08 $30.00
www.brjpharmacol.org

RESEARCH PAPER

# Effect of CCR5 receptor antagonists on endocytosis of the human CCR5 receptor in CHO-K1 cells

J Longden[1,2,3], E-L Cooke[2,4] and SJ Hill[1]

[1]*Institute of Cell Signalling, Medical School, Queens Medical Centre, Nottingham, UK and* [2]*Advanced Science and Technology Laboratory, AstraZeneca Research and Development Charnwood, Loughborough, Leicestershire, UK*

**Background and purpose:** The CCR5 chemokine receptor is a member of the G protein-coupled receptor (GPCR) family that is expressed by macrophages, memory T-lymphocytes and dendritic cells and is activated by chemotactic proteins (e.g. MIP-1α [CCL3], MIP-1β [CCL4] and RANTES [CCL5]). CCR5 is also the principal co-receptor for macrophage-tropic strains of human immunodeficiency virus-1 (HIV-1) and some chemokines can inhibit HIV-1 infection by stimulating CCR5 receptor endocytosis. The aim of this study was to evaluate the effect of CCR5 antagonists on CCR5 endocytosis.
**Experimental approach:** The effects of CCR5 agonists and antagonists on receptor internalization in CHO cells, expressing a C-terminal green fluorescent protein-tagged human CCR5 receptor (CCR5-GFP), were quantified using a confocal imaging plate reader.
**Key results:** MIP-1α [CCL3], MIP-1β [CCL4] and RANTES [CCL5] were all able to stimulate potently the internalization of CCR5-GFP. This effect was inhibited by the non-peptide antagonist TAK 779. The CCR5 peptide antagonist met-RANTES antagonized MIP-1α-mediated increases in intracellular free calcium but was also able to stimulate a substantial internalization of the human CCR5-GFP receptor. However, CHO cells exhibited an aminopeptidase activity that was able to metabolize sufficient met-RANTES into an agonist metabolite capable of stimulating calcium mobilization via CCR5 receptors in naïve cells.
**Conclusions and implications:** These data suggest that there is an endogenous aminopeptidase activity on the surface of CHO cells, that produces a slow internalization of the receptor following a time-dependent conversion of receptor-bound met-RANTES from a CCR5 receptor antagonist into a CCR5 agonist molecule.
*British Journal of Pharmacology* (2008) **153,** 1513–1527; doi:10.1038/sj.bjp.0707691; published online 28 January 2008

**Keywords:** receptor internalization; CCR5 receptor; met-RANTES; G-protein-coupled receptors; antagonist stimulated; endosomes; aminopeptidase

**Abbreviations:** CCL, official chemokine ligand nomenclature name; CHO, Chinese hamster ovary; GFP, green fluorescent protein; GPCR, G-protein-coupled receptor; HIV-1, human immunodeficiency virus, type 1; MAP kinase, mitogen-activated protein kinase; MIP, macrophage inflammatory protein; PBS, phosphate-buffered saline; RANTES, released on activation normal T cell expressed and secreted

## Introduction

The CCR5 chemokine receptor is a member of the G-protein-coupled receptor (GPCR) family that is expressed by macrophages, memory T lymphocytes and dendritic cells (Kazmierski *et al.*, 2003; Rot and von Andrian, 2004; Johnson *et al.*, 2005). It is activated by a large family of chemotactic proteins (chemokines, for example, macrophage inflammatory protein (MIP)-1α (CCL3), MIP-1β (CCL4) and released on activation normal T cell expressed and secreted (RANTES) (CCL5)), which are secreted by many cell types to regulate leukocyte activation and recruitment leading to inflammatory responses (Rot and von Andrian, 2004). CCR5 is also the principal co-receptor for macrophage-tropic strains of human immunodeficiency virus, type 1 (HIV-1) and acts in concert with CD4 to facilitate viral entry into cells (Simmons *et al.*, 2000; Kazmierski *et al.*, 2003). A number of chemokines and small molecule receptor antagonists can inhibit HIV-1 infection *in vitro* by blocking the binding of the viral envelope protein glycoprotein gp120 to CCR5 (Simmons *et al.*, 2000). Alternatively, some of these chemokines may also induce CCR5 receptor endocytosis and consequently decrease the cell surface availability of CCR5 for interaction with the viral envelope proteins (Mack *et al.*, 1998; Signoret *et al.*, 2000).

Correspondence: Professor SJ Hill, Institute of Cell Signalling, Medical School, Queen's Medical Centre, University of Nottingham, Nottingham NG7 2UH, UK.
E-mail: stephen.hill@nottingham.ac.uk
[3]Current address: Eskitis Institute of Cell and Molecular Therapies, Griffith University, Nathan, Queensland 4111, Australia.
[4]Current address: Cancer BioScience, AstraZeneca Research and Development Boston, 35 Gatehouse Drive, Waltham, MA 02451, USA.
Received 12 September 2007; revised 6 November 2007; accepted 4 December 2007; published online 28 January 2008

The mechanisms underlying endocytosis of GPCRs have largely been determined as a consequence of extensive studies with the prototypical GPCR, the $\beta_2$-adrenoceptor (Carman and Benovic, 1998; Ferguson *et al*., 1998; Marchese *et al*., 2003). Agonist activation of GPCRs leads to phosphorylation of the intracellular C terminus or third intracellular loop of the receptor by second-messenger-dependent protein kinases and GPCR kinases (Barak *et al*., 1997; Carman and Benovic, 1998; Ferguson *et al*., 1998; Kahout and Lefkowitz, 2003; Marchese *et al*., 2003). This in turn leads to the binding of non-visual arrestins to the receptor (Barak *et al*., 1997; Ferguson *et al*., 1998). Binding of arrestin causes a disruption of the receptor G-protein interactions and prevents further signalling from the receptor via the G protein (Barak *et al*., 1997). In addition, the arrestins act as adaptor proteins coupling many GPCRs to clathrin-coated pits and targeting the receptor for subsequent internalization (Luttrell and Lefkowitz, 2002; Marchese *et al*., 2003).

Studies have demonstrated that, in addition to their well-characterized role in GPCR internalization, arrestins also have a broader signalling role, can act as scaffolds for activation of mitogen-activated protein (MAP) kinase cascades by GPCRs and can function to retain activated MAP kinase enzymes within the cytosol, rather than allowing them to translocate to the nucleus and stimulate gene transcription (Luttrell *et al*., 2001; Seta *et al*., 2002; Tohgo *et al*., 2002; Wei *et al*., 2003). Furthermore, it is now clear that this interaction between GPCRs and arrestins can activate intracellular signalling via MAP kinase independently of the involvement of heterotrimeric G proteins (Seta *et al*., 2002; Azzi *et al*., 2003; Wei *et al*., 2003; Terrillon and Bouvier, 2004).

However, stimulation of interactions between GPCRs and arrestins is not exclusively mediated by receptor agonists. There is increasing evidence that the nature of the receptor–arrestin interaction may not be entirely dependent upon agonist-stimulated receptor phosphorylation. For example, Azzi *et al*. (2003) have recently reported that certain β-adrenoceptor inverse agonists can stimulate MAP kinase activation in a β-arrestin-dependent manner in HEK 293 cells overexpressing the $\beta_2$-adrenoceptor. Furthermore, a number of receptor antagonists have also been shown to stimulate internalization of 5-$HT_{2A}$ and cholecystokinin type A receptors in the absence of any measurable agonist activity (Roettger *et al*., 1997; Gray and Roth, 2001). These latter data suggest that receptor internalization can occur in the absence of receptor phosphorylation.

To monitor the process of GPCR internalization, it is important to be able to visualize the location of the receptor using specific antibodies or recombinant attachment to the receptor of a fluorescent probe, such as green fluorescent protein (GFP) (Tarasova *et al*., 1997; Zhang *et al*., 1999; Conway *et al*., 2001). However, simple visualization of receptors using confocal microscopy can suffer from inherent bias in the selection of appropriate fields of view. In the present study, we have used a confocal imaging plate reader to undertake a quantitative analysis of the effects of CCR5 agonists and antagonists on receptor internalization. This new approach provides a means by which the extent of internalization can be quantified, not only in terms of the proportion of cells responding, but also the number of intracellular vesicles containing GFP-tagged CCR5 receptor within each cell and the fluorescence intensity of these receptor proteins within these vesicles.

## Materials and methods

*Cells and vectors*

Flp-In Chinese hamster ovary (CHO) cells and the pcDNA5-FRT vector were purchased from Invitrogen (Paisley, UK). The EGFP-N1 was purchased from Clontech (Oxford, UK) and the human CCR5 receptor was kindly provided by AstraZeneca R&D (Alderley Park, Cheshire, UK).

*Materials*

FuGENE 6 was purchased from Roche (Burgess Hill, West, Sussex, UK), all chemokines and the CCR5 primary antibody were from R&D Systems (Abingdon, UK). Fluo4, Pluronic F-127, Hoechst 33342 and BODIPY FL $C_5$-ceramide were from Molecular Probes (Paisley, UK). All other chemicals were from Sigma (Gillingham, Dorset, UK).

*Construction of the CCR5 receptor-GFP expression vector*

The human CCR5 receptor (GenBank NM 000579) in pcDNA3 was amplified by PCR to insert a kozac sequence and a *Hin*dIII restriction site at the 5′ end and to remove the stop codon and insert a *Bam*HI restriction site at the 3′ end of the gene. The primers used were 5′-AGTCAAGCTTACCAC CATGGATTATCAAGTGTCAAGTCC-3′ and 5′-AGTCGGATC CAAGCCCACAGATATTTCCT-3′. The pEGFP-N1 was then mutated to transform the start codon on the GFP gene to a serine. The two primers used were 5′-CCGGTCGCCACCTCC GTGAGCAAGGGC-3′ and 5′-GCCCTTGCTCACGGAGGTGG CGACCGG-3′. The modified CCR5 and GFP genes were then cleaved from their respective vectors (using *Hin*dIII and *Bam*HI for CCR5 and *Bam*HI and *Not*I for GFP) and ligated into *Hin*dIII–*Not*I-digested pcDNA5-FRT. All receptor constructs were sequenced on both strands using automated fluorescent sequencing (University of Nottingham).

*Generation of CHO cell line stably expressing CCR5-GFP*

Flp-In CHO cells were grown to 80% confluency in a six-well plate in Ham's F-12 media containing 10% fetal bovine serum (FBS) and 1 mM L-glutamine. Transfection was carried out in Optimem media using 3 μl of FuGENE 6 reagent and 1 μg of plasmid DNA per well. Positive cells were selected using the antibiotic hygromycin at 200 $\mu g\,ml^{-1}$ (in Ham's F-12 media containing 10% FBS) as a selection marker. The transfected cell line was then sorted by fluorescence-activated cell sorter on the basis of the GFP expression using a Beckman Coulter Epics Altra to create a clonal cell line. GFP-expressing cells were sorted into 96-well plates (one cell per well) and screened on a GE Healthcare IN Cell Analyser 3000 plate reader (see below) to identify clones with uniform levels of receptor expression. Cells were routinely passaged

through Ham's F-12, 10% FBS, 200 μg ml$^{-1}$ hygromycin and 1 mM L-glutamine.

*Measurement of intracellular free [$Ca^{2+}$]*

Cells were seeded onto black 96-well Packard ViewPlates at a concentration of 10 000 cells per well and grown in Ham's F-12 growth media containing 10% FBS and 1 mM L-glutamine at 37 °C for 48 h. For the last 24 h of this time period, cells were grown in Ham's F-12 medium without FBS. Cells were then incubated in loading buffer (Hank's balanced salt solution (HBSS) with 20 mM HEPES, 2.5 mM probenecid and 2.2 μM Fluo4-AM, premixed with Pluronic F-127, 0.2% final concentration) at 37 °C for 60 min. The loading buffer was aspirated from the wells and replaced with 30 μl of HBSS with HEPES and probenecid. The plate was then transferred onto a Molecular Devices fluorometric imaging plate reader (FLIPR3) and imaged for 8 s (one image s$^{-1}$) to take a baseline reading, then imaged for a further 2 min (60 reads) to measure response to ligand. Ligands were diluted in Hank's–HEPES buffer in a Matrix Screenmate 96-well plate, and 30 μl of the ligand solution was transferred into the cell plate after the eighth image. The antagonist pretreatment assays were performed as described above with one exception; loading buffer was aspirated from the wells and replaced with 30 μl of 1000 nM chemokine diluted in Hank's-HEPES buffer, rather than 30 μl of buffer alone. The chemokines were incubated with the cells for 30 min at 37 °C before being imaged on the FLIPR3 as described above.

*Receptor internalization assay*

Cells were seeded onto 96-well black Packard ViewPlates at a concentration of 10 000 cells per well and grown at 37 °C for 48 h. For the last 24 h of this time period, cells were grown in Ham's F-12 medium without FBS. For the concentration–response assays, cells were treated with 50 μl of various concentrations of chemokines for 60 min at 37 °C, before being fixed with 50 μl 4% paraformaldehyde (in phosphate-buffered saline (PBS)), that is, 2% final, for 20 min. The cells were then washed, once with PBS, and stained with 0.5 μM Hoechst 33342 for 20 min.

For the time-course assays, cells were treated with 50 μl of either 100 nM MIP-1α or 1 μM met-RANTES before being fixed and stained with Hoechst as described above. For the antagonist pretreatment and experiments using filipin, sucrose, acetic acid or angiotensin IV, cells were incubated at 37 °C with 50 μl of 1 μM chemokine, 1 μg ml$^{-1}$ filipin, 0.4 M sucrose, 5 mM acetic acid (pH = 5) or 1 mM angiotensin IV for 30 min (5 min in the case of acetic acid); 50 μl of MIP-1α (CCL3) or met-RANTES (diluted in HBSS at double the required concentration) was then added to the cells and incubated for 60 min at 37 °C, before being fixed and stained as described above.

After Hoechst staining, cells were washed (once with PBS) and imaged on the GE Healthcare IN Cell Analyser 3000 in PBS. For each well, one image (0.745 mm$^2$ in area) was captured using a ×40 objective with a 364 nm excitation line and 438.5–462.5 nm band-pass filter (for the Hoechst) and a 488 nm excitation line and 512.5–557.5 nm band-pass filter (for the CCR5-GFP receptor).

Before each set of experiments, a '*z*-stack' of images was captured using the IN Cell Bead Analysis Module to determine the optimum focal plane. Nine images of the cells were taken, in 1.00-μm intervals, starting from −4.00 μm (the distance the image is captured from the liquid–solid interface layer detected by the autofocus laser) and images were examined by eye for optimum focus.

A 'flat-field' solution was also used in all experiments to correct for excitation intensity differences across the well (the laser excitation is brightest in the centre of the well). The flat-field comprised three dyes, Alexa 350, fluorescein and Cy5, which were scanned prior to the data images. The IN Cell software detected fluctuations in emission intensity across the well; correction factors were then applied automatically to subsequent images to reproduce approximately the effect of even excitation.

Neutral density filters were applied to the flat field and sampled to make sure that the emission counts generated were between 300 and 3000 (the charge-coupled device cameras are less sensitive operating outside this range). The neutral density filters used in all assays were 1 (which blocks 90% of the excitation source) on the blue and u.v. excitation sources and 0 (which blocks 0% of the excitation source) on the red excitation source. The flat-field solution concentrations corresponding to these neutral density filters were 3 μl of 1.2 nM Alexa 350, 0.5 μl of 314 μM fluorescein and 0.5 μl of 1 mg ml$^{-1}$ Cy5 all diluted in 150 μl of PBS.

*Live cell internalization assay*

Cells were seeded onto 96-well black Packard ViewPlates at a concentration of 10 000 cells per well and grown at 37 °C for 48 h. For the last 24 h of this time period, cells were grown in Ham's F-12 medium without FBS. The cells were then stained with 0.5 μM Hoechst 33342 for 20 min, washed once (with HBSS), treated with chemokine (either 100 nM MIP-1α (CCL3) or 1 μM met-RANTES) and then imaged on the Amersham IN Cell Analyser 3000 in HBSS.

The environmental chamber of the IN Cell Analyser 3000 was pre-equilibriated to 37 °C, 5% $CO_2$ and 75% humidity; and for each well, images (0.745 mm$^2$ in area) were captured every 10 min for 90 min using a ×40 objective with a 364 nm excitation line and 438.5–462.5 nm band-pass filter (for the Hoechst) and a 488 nm excitation line and 512.5–557.5 nm band-pass filter (for the CCR5-GFP receptor). Plates were sealed with a Greiner Breathe-Easy seal to minimize evaporation.

*Antibody labelling assay for wild-type CCR5 receptors*

Cells expressing the wild-type CCR5 receptor were seeded onto Packard ViewPlates as described for the receptor internalization assay. On the following day, cells were blocked for 1 h at 37 °C in blocking buffer (HBSS containing 2% goat serum and 2% BSA). Cells were then incubated with primary antibody (diluted 1:200 in blocking buffer) for 1 h at 37 °C, after which the antibody was washed out with HBSS and cells were treated with 50 μl of 100 nM MIP-1α or 1 μM

met-RANTES (diluted in HBSS) for the required time period. Cells were fixed with 50 μl 4% paraformaldehyde for 20 min at room temperature before being made permeable with 0.2% Triton X-100 (diluted in PBS) for 10 min, and stained with Alexa Fluor 633 goat anti-mouse (diluted 1:200 in blocking buffer) for 45 min at room temperature. Cells were then washed once in PBS and stained with Hoechst 33342 (0.5 μM for 20 min).

For each well, one image (0.745 $mm^2$ in area) was captured using a $\times 40$ objective with a 364 nm excitation line and 438.5–462.5 nm band-pass filter (for the Hoechst) and a 633 nm excitation line and 667.5–722.5 nm band-pass filter (for the Alexa Fluor 633 secondary antibody).

*Confocal microscopy*

Chinese hamster ovary cells expressing the human CCR5 receptor tagged with GFP were plated in Nunc eight-well chamber slides at a concentration of 30 000 cells per well and grown at 37 °C for 48 h. For the last 24 h of this time period, cells were grown in Ham's F-12 medium without FBS. For the Golgi marker experiments, cells were incubated with chemokine, either 100 nM MIP-1α (CCL3) or 1000 nM met-RANTES (diluted in HBSS) for 60 min at 37 °C. Subsequently, cells were washed once with HBSS and incubated on ice for 30 min with BODIPY FL $C_5$-ceramide (5 μM) to label the extracellular surface of the cells. The cells were then washed in ice-cold HBSS and incubated for 30 min at 37 °C. Confocal microscopy was performed at room temperature on a Zeiss LSM 510 laser scanning microscope with a Zeiss Plan-Apo $\times 63$ 1.4 NA oil immersion objective using multitracking. A 488 nm excitation line was used with a 505–530 nm band-pass filter (for the CCR5-GFP receptor) and a 560 nm long-pass filter (for BODIPY FL $C_5$-ceramide). Colocalization was determined using the Zeiss LSM 510 software.

*Measurement of endogenous aminopeptidase activity in CHO-CCR5-GFP cells*

CHO-CCR5-GFP cells were grown to confluence in 96-well plates. The medium was removed and the cells were washed twice with 200 μl PBS. The medium was then replaced with 200 μl PBS containing different concentrations of L-leucine-*p*-nitroanilide and incubated at 37 °C for 60 min. The formation of *p*-nitroaniline was then monitored by measuring the absorption at 405 nm using a Dynex MRX II plate reader.

*Data analysis*

Receptor internalization was quantitated using the IN cell granularity analysis algorithm. This algorithm determined properties of individual objects (usually a single cell) detected by applying a user-generated threshold to the intensity of the nuclear marker channel (the blue fluorescence channel). The threshold for intensity was set on a per assay basis and was corrected for background fluorescence in the image.

Once the objects were defined, these were eroded by application of another user-generated filter (to create a more distinct nuclear edge), which discards 20% of the pixels (those with the lowest intensity) within the object. The software also automatically records the size of the object and a final user-generated filter was applied to exclude objects above and below a defined area. The filter used in these experiments discarded objects below $9 \times 9$ (equivalent to approximately 0.3 of a cell), and above $60 \times 60$ (equivalent to approximately 2 cells) pixels in area.

Cell nuclei were detected as described using the Hoechst 33342 staining (Figure 1) and a box, $\sim 40 \times 40$ pixels (termed the cytoplasmic box), was created, with the nucleus at the centre, to define the maximum area of a single cell. Within this box, the analysis algorithm identified 'grains' based upon the predetermined size of a grain and its fluorescence intensity (Figure 1). The brightest pixel within the cytoplasmic box was defined as the centre of a grain and a grain box of a particular size set around the brightest pixel. Two grain box sizes were used in the present study: $9 \times 9$ pixels (for large grains) and $3 \times 3$ pixels (for small grains). In each case, an outer box was also created around the large ($17 \times 17$ pixels) or small ($9 \times 9$ pixels) grain boxes (see Figures 1e and f). The fluorescence intensity within the grain box was compared with the surrounding pixels (in the outer box) and if it did not exceed the threshold set, the grain was discarded. This process was repeated within each cytoplasmic box as many times as possible. The influence of different drug treatments on the number (N-grains) and fluorescent intensity (F-grains) of large and small grains in each cell was then determined. Values are expressed as mean ± s.e.mean and $n$ refers to the number of separate experiments performed.

Agonist concentration–response curves were fitted using the program Prism 2 (GraphPad Software) to the logistic equation:

$$\text{Response} = \frac{E_{MAX}\,\text{x}\,[\text{A}]^{n_H}}{\left([\text{A}]^{n_H} + \text{EC}_{50}^{n_H}\right)}$$

where $E_{MAX}$ is the maximal response, [A] is the agonist concentration, $EC_{50}$ is the concentration of agonist producing 50% of the maximal response and $n_H$ is the Hill coefficient. All data are presented as mean ± s.e.mean of at least three separate experiments. The $n$ refers to the number of separate experiments. The data for the time-course studies were fitted to the equation:

$$\text{Response} = C + (Y_{MAX} - C)\ (1 - \exp(-kt))$$

where $C$ is the extent of internalization at time zero, $Y_{MAX}$ is the maximum level of ligand-stimulated internalization, $t$ is the time point and $k$ is the rate constant for association. The $t_{1/2}$ was calculated as $0.69k^{-1}$.

## Results

*Agonist-induced internalization of CCR5 to large perinuclear grains*

Trafficking of the human CCR5-GFP receptor to the perinuclear region of individual cells was quantified using a granularity analysis algorithm as described above. This detected large perinuclear focal spots (large perinuclear

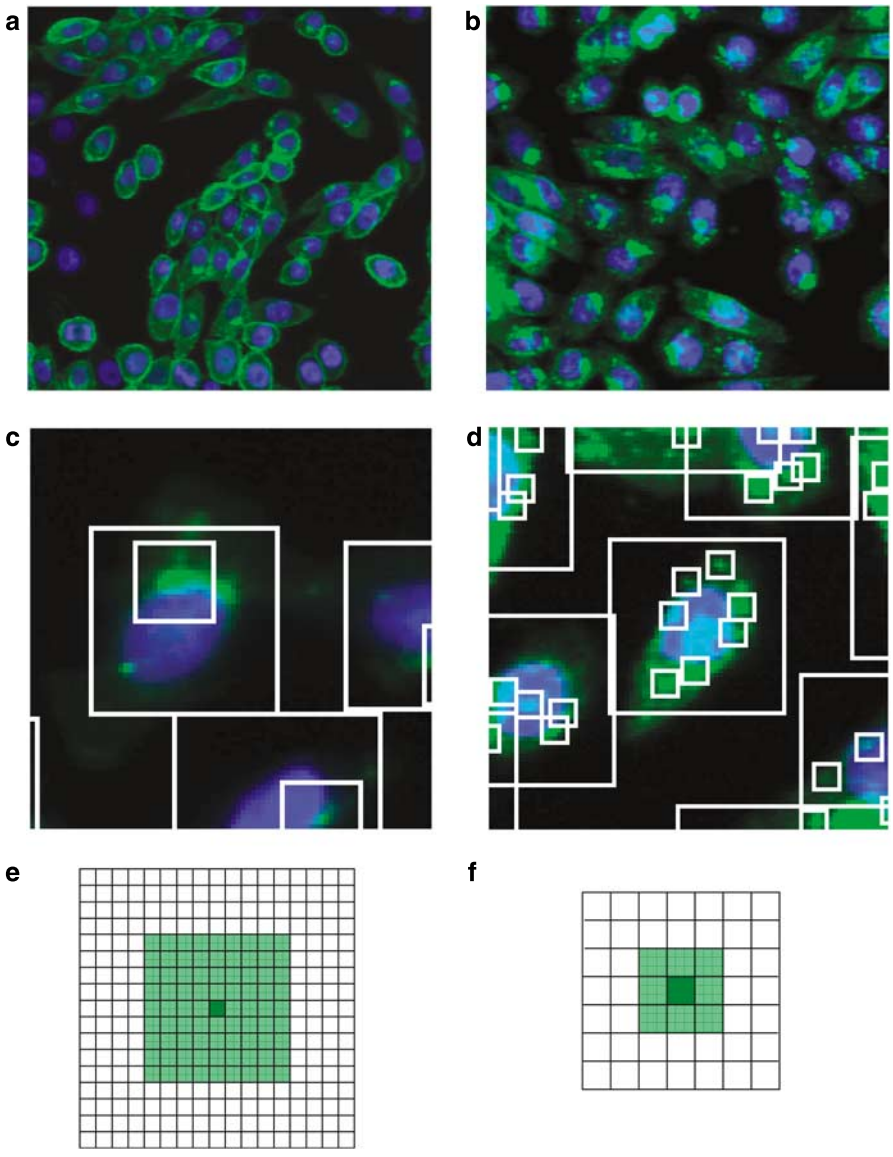


**Figure 1** Analysis of MIP-1α (CCL3)-induced internalization of CCR5-GFP (green fluorescent protein) receptors using the IN cell granularity analysis algorithm. Examples of images from a single control (**a**) or MIP-1α-stimulated (**b**; 100 nM; 60 min) well are shown. Cell nuclei were stained with Hoechst 33342 dye (blue) and a box (termed the cytoplasmic box, approximately 40 × 40 pixels) was created to define the maximum area of a single cell (large boxes in **c**, **d**). Within this box, the analysis algorithm then identified large (**c**) and small grains (**d**). In each case, the brightest green pixel within the cytoplasmic box was detected and defined as the centre of a grain. The algorithm then established a grain box of either 9 × 9 pixels (large grains) or 3 × 3 pixels (for small grains). In each case, an outer box was then created around the large (17 × 17 pixels; **e**) or small (7 × 7 pixels; **f**) grain boxes. Within the grain box, the fluorescence intensity of the grain was compared with the surrounding pixels (in the outer box) and if it exceeded the threshold set, the grain was accepted.

grains) within each cell, which had pronounced fluorescence intensity differences compared with the surrounding regions of the cell (Figure 1). For each well of a 96-well plate, the fluorescence characteristics of *circa* 1000 cells were automatically monitored (Figures 2a and c). In general, only one large perinuclear grain was detected within a given cell, although occasionally two were present. Figure 2a shows the distribution of the fluorescence intensities of these large perinuclear grains for a single well from unstimulated control cells. The large number of cells at zero fluorescence intensity represents cells with no large perinuclear spot. Following stimulation for 60 min with 100 nM MIP-1α (CCL3), there was a pronounced shift in the distribution to higher fluorescence intensities and a marked decrease in the number of cells without a measurable perinuclear fluorescent grain (Figure 2a). However, the finding that 155 cells (in the presence of 100 nM MIP-1α) of a total of 1172 cells in a representative well (that is, 13.2%) did not show the appearance of a large perinuclear grain of CCR5-GFP fluorescence emphasizes the importance of an automated and quantitative approach to measurement of receptor internalization. To quantify the changes induced by an agonist in the internalization of the CCR5-GFP receptor to this perinuclear grain, the mean fluorescent intensity per cell was determined. MIP-1α (100 nM) produced a time-dependent stimulation of receptor internalization into the large

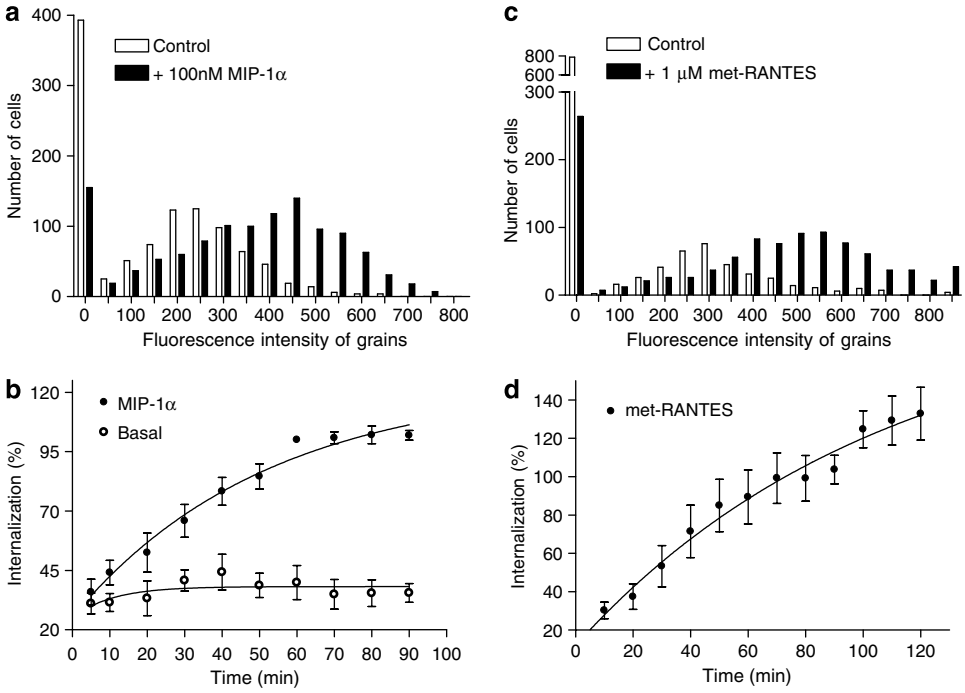


**Figure 2** Increase in the fluorescent intensity of CCR5-GFP (green fluorescent protein) receptors in large intracellular perinuclear grains following stimulation with macrophage inflammatory protein (MIP)-1α (CCL3, **a**, **b**) or met-RANTES (released on activation normal T cell expressed and secreted) (**c**, **d**). (**a**, **c**) The frequency distribution of cells within a particular intensity range (for large grains) in a single well of control cells (vehicle only addition) and MIP-1α (**a**; 100 nM; 60 min) or met-RANTES (**c**; 1 μM; 60 min)-stimulated cells. The total number of cells analysed in each well was 1046 (**a**; control), 1172 (**a**; MIP-1α), 1167 (**c**; control) and 1068 (**c**; met-RANTES). The degree of CCR5-GFP internalization induced at different times following cell stimulation (mean fluorescence intensity expressed as a percentage of the response to 100 nM MIP-1α at 60 min, which was measured in each experiment) in response to 100 nM MIP-1α and 1 μM met-RANTES is shown in (**b**) and (**d**), respectively. Values (mean ± s.e.mean) are from three (basal; **b**), six (MIP-1α, **b**) and six (met-RANTES, **d**) separate experiments. Please note that in (**b**, **d**) the ordinate does not begin at zero.

perinuclear grains, with an estimated $t_{1/2}$ of 23.65 ± 1.46 min (Figure 2b; $n = 5$). This internalization response to MIP-1α was concentration dependent (log $EC_{50} = -9.03 \pm 0.10$; $n = 10$; Figure 3a) and was also seen with MIP-1β (CCL4; log $EC_{50} = -8.24 \pm 0.03$; 91.25 ± 3.32% of MIP-1α maximum; $n = 9$) and RANTES (CCL5; log $EC_{50} = 8.66 \pm 0.04$; 83.05 ± 4.32% of MIP-1α maximum; $n = 9$).

*Influence of peptide CCR5 antagonists on CCR5 internalization*

The CCR5 receptor peptide antagonists vMIP-II, met-RANTES (Figure 3c; 1 μM), eotaxin-3 and MCP-3 (CCL7; data not shown; 1 μM) were all able to antagonize markedly the mobilization of intracellular calcium stimulated by MIP-1α in CHO cells expressing the human CCR5-GFP receptor (Figure 3c). However, pretreatment of CCR5-GFP cells with each antagonist (1 μM) did not produce the expected large rightward shift in the concentration–response curve for MIP-1α-induced receptor internalization (Figure 3a). Only vMIP-II was able to produce any antagonism of the MIP-1α response, shifting the MIP-1α concentration–response curve from a log $EC_{50}$ of 9.03 ± 0.10 to −8.74 ± 0.10 ($n = 6$; Figure 3a). In marked contrast, the small molecule, non-peptide CCR5 antagonist TAK 779 (Baba *et al*., 1999) was able to produce a potent antagonism of the MIP-1α-stimulated CCR5-GFP receptor internalization (Figure 3b).

Pretreatment for 30 min with met-RANTES caused a cumulative increase in the MIP-1α response, which was not consistent with simple competitive antagonism (Figure 3a). Furthermore, met-RANTES alone was able to produce a substantial internalization of the CCR5-GFP receptor over 30–120 min (Figures 2c and d, and 3d). This effect of met-RANTES was concentration dependent and induced at low concentrations of the CCR5 antagonist (log $EC_{50} = -8.66 \pm 0.04$; $n = 4$; Figure 3d). The stimulation of CCR5-GFP receptor internalization by met-RANTES was completely inhibited by TAK 779 and revealed a small concentration-dependent inhibition of basal receptor internalization by met-RANTES (Figure 3d).

However, vMIP-II, eotaxin-3 (CCL26) and MCP-3 (CCL7) alone produced no significant stimulation of receptor internalization at concentrations up to 600 nM (data not shown). At 1 μM, vMIP-II, eotaxin-3 and MCP-3 did stimulate CCR5-GFP receptor internalization (by 37.55 ± 4.53, 47.48 ± 17.16 and 73.00 ± 4.43%, respectively, of the maximum effect of MIP-1α; $n = 3$), although this might be a nonspecific effect at such high concentrations (data not shown).

*Influence of filipin and acidification of the cell cytosol on agonist- and antagonist-induced internalization*

To investigate the pathway used for CCR5-GFP receptor internalization in response to MIP-1α and met-RANTES, the effect of hypertonic sucrose (which inhibits clathrin-mediated internalization; Heuser and Anderson, 1989),

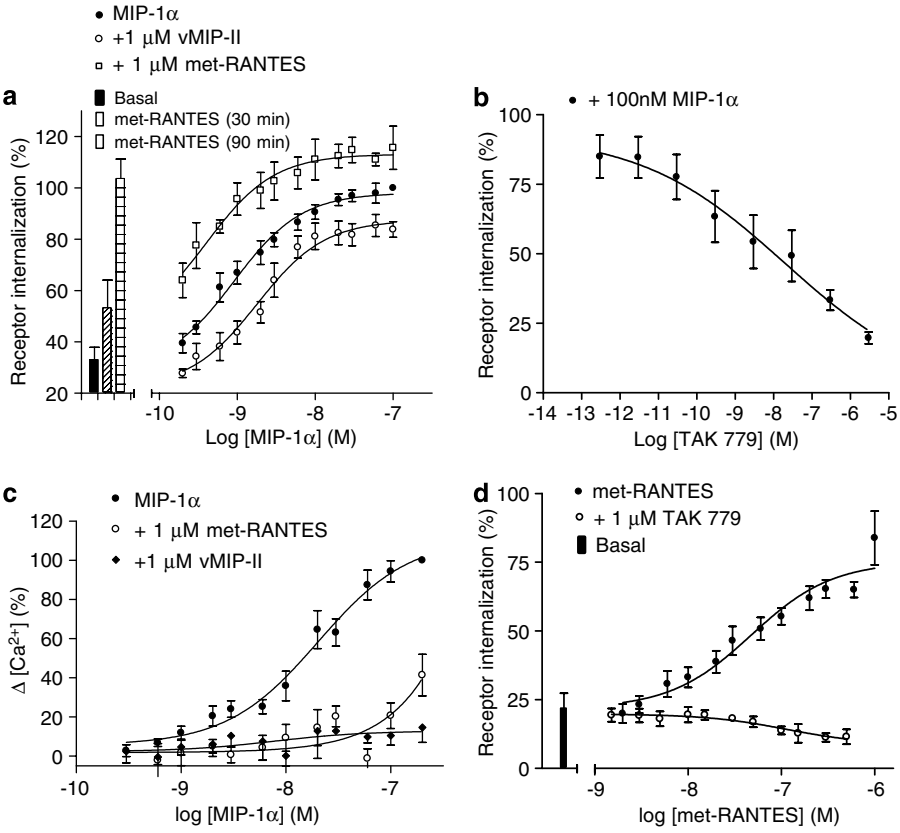


**Figure 3** Influence of met-RANTES (released on activation normal T cell expressed and secreted), vMIP-II and TAK 779 on macrophage inflammatory protein (MIP)-1α (CCL3)-induced internalization of CCR5-GFP (green fluorescent protein) receptors into large intracellular perinuclear focal spots and calcium mobilization. Receptor internalization was measured using an IN Cell Analyser 3000 and the large grain granularity algorithm as described in Materials and methods. met-RANTES, vMIP-II (**a**; both at 1 μM) and TAK 779 (**b**) were applied to cells 30 min prior to addition of MIP-1α. The mean population fluorescence intensity of grains per cell was calculated and expressed as a percentage of the response to 100 nM MIP-1α at 60 min. In each individual experiment, four replicate determinations were made for each condition. Values represent mean ± s.e.mean of nine (MIP-1α alone), four (MIP-1α + met-RANTES), six (MIP-1α + vMIP-II) and six (TAK 779) separate experiments. (**c**) Effect of MIP-1α and chemokine receptor antagonists on mobilization of intracellular calcium in Chinese hamster ovary (CHO)-CCR5-GFP cells. met-RANTES (1 μM) or vMIP-II (1 μM) was added 30 min prior to addition of MIP-1α. Intracellular levels of calcium were monitored in Fluo4-loaded cells using a fluorometric imaging plate reader (FLIPR3). Values are expressed as a percentage of the maximum response to 100 nM MIP-1α in the absence of antagonist. In each individual experiment, four replicate determinations were made for each condition. Values shown are mean ± s.e.mean from three separate experiments. (**d**) Concentration–response characteristics of the CCR5-GFP internalization into large perinuclear grains induced by met-RANTES. Mean fluorescence intensity values are expressed as a percentage of the response to 100 nM MIP-1α at 60 min, which was measured in each experiment. Panel a, Concentration–response curves to met-RANTES in the presence or absence of TAK 779 (1 μM). In each individual experiment, four replicate determinations were made at each concentration. Values shown are mean ± s.e.mean from four (met-RANTES alone) and three (met-RANTES + TAK 779) separate experiments. Please note that in (**a**) the ordinate does not begin at zero.

filipin (which inhibits lipid raft- and caveolae-mediated internalization; Orlandi and Fishman, 1998) and cytosolic acidification (which inhibits dynamin-mediated production of clathrin-coated vesicles; Sandvig *et al*., 1987) on these responses was investigated. Filipin did not attenuate MIP-1α-induced CCR5-GFP receptor internalization (Figure 4), but 0.4 M sucrose proved to be cytotoxic to this particular cell line (data not shown). As an alternative strategy to investigate the role of clathrin-coated pits, the effect of 5 mM acetic acid at pH 5 was investigated. This approach takes advantage of the ability of a weak acid such as acetic acid to penetrate the cell membrane rapidly in its undissociated form and to dissociate in the cytosol to lower the cytosolic pH (Sandvig *et al*., 1987). This protocol completely attenuated the endocytosis of the CCR5-GFP receptor in response to either MIP-1α or met-RANTES (Figure 4). There was no effect of acetic acid when applied at pH 7 (at which pH the acetic acid is dissociated) or of simple acidification of the extracellular medium with HCl (pH 5), which confirmed the mechanism of action of acetic acid (Figure 4) suggested by Sandvig *et al*. (1987). The identity of the large perinuclear focal location of the internalized CCR5 receptor in the large grains remains to be confirmed, but colocalization studies with BODIPY FL $C_5$-ceramide suggest that it is likely to be the Golgi apparatus (Figure 5).

### *Internalization of the wild-type CCR5 receptor by MIP-1α and met-RANTES*

To establish whether the C-terminal GFP tag is influencing the extent and time course of the internalization response to met-RANTES, studies with the wild-type receptor were also performed. In these experiments, the location of the CCR5 receptor was determined using an antibody to an epitope in

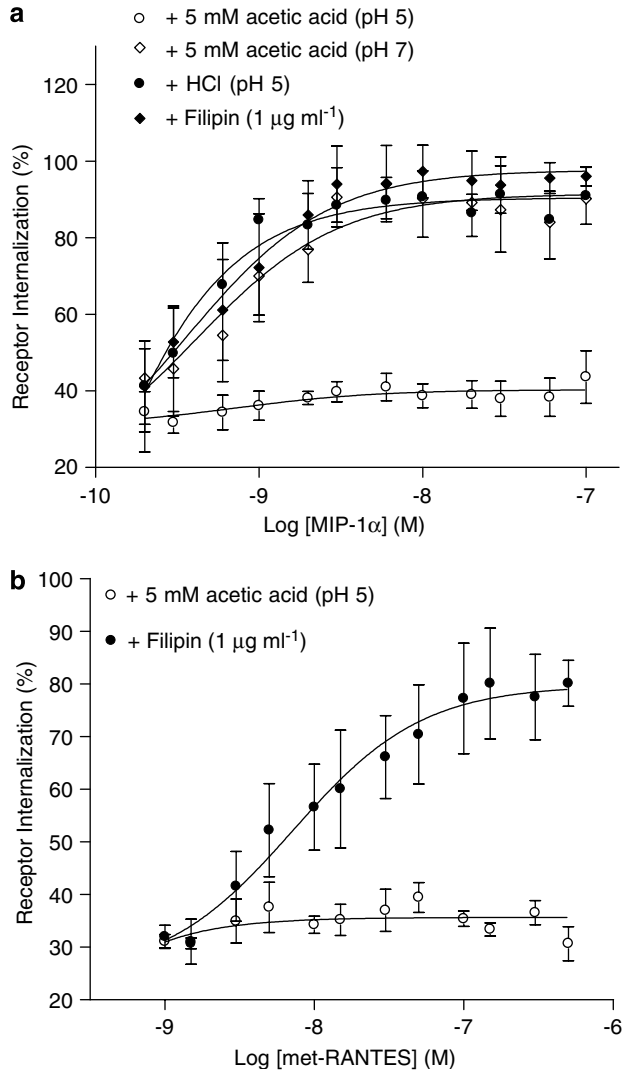


**Figure 4** Influence of filipin and cytosol acidification on the internalization of CCR5-GFP (green fluorescent protein) induced by (**a**) macrophage inflammatory protein (MIP)-1α (CCL3) and (**b**) met-RANTES (released on activation normal T cell expressed and secreted). Filipin (1 mg ml$^{-1}$) was added 30 min prior to addition of MIP-1α or met-RANTES. Addition of acetic acid (pH 5 or 7) and simple acidification of cells with HCl (pH 5) was carried out 5 min prior to addition of MIP-1α or met-RANTES. In each individual experiment, four replicate determinations were made at each concentration. Values shown are mean ± s.e.mean from 3–4 (MIP-1α; 4 experiments were carried out with acetic acid at pH 5, the others were $n=3$) or 3 (met-RANTES) separate experiments. Mean fluorescence intensity values are expressed as a percentage of the maximum response to 100 nM MIP-1α alone, which was measured in each experiment. Please note that in (**a**, **b**) the ordinate does not begin at zero.

the N terminus of the CCR5 receptor. It was found that met-RANTES stimulated CCR5 receptor internalization with a similar time course, and to a similar extent, as that observed with the CCR5-GFP receptor variant (Figure 6).

*Effect of CCR5 agonists and antagonists on internalization into endosomal small vesicles*

Live cell imaging of the time course of CCR5-GFP receptors in response to either MIP-1α or met-RANTES (Figure 7) indicated that a marked internalization of the receptor into small vesicles preceded the appearance of CCR5-GFP in large perinuclear grains. To gain insight into the quantitative nature of this effect of CCR5 agonists and antagonists on endocytosis of the receptor into small endosomal vesicles (Lim *et al*., 2001), the confocal images were also analysed for the presence of small grains (see Materials and methods) using the granularity algorithm of the In Cell Analyser 3000. MIP-1α produced a time-dependent increase in both the number (small N-grains $t_{1/2}=10.42\pm2.07$ min; $n=5$) and fluorescence intensities (small F-grains; $t_{1/2}=23.06\pm5.55$ min; $n=5$) of CCR5-GFP receptors in small grains within cells (Figure 10). As shown in Figure 8, this was a faster process than the increased fluorescence in large perinuclear grains (Figure 2). MIP-1α (N-grain log $EC_{50}=-8.75\pm0.18$; F-grain $EC_{50}=-8.91\pm0.21$; $n=10$), MIP-1β (log $EC_{50}=-8.19\pm0.09$; $-8.42\pm0.28$; $n=9$) and RANTES ($EC_{50}=-8.32\pm0.21$; $-8.35\pm0.12$; $n=9$) produced concentration-dependent increases in both small N-grains and small F-grains, respectively (Figure 9). Similarly, met-RANTES was able to produce a concentration-dependent increase in the number (log $EC_{50}=-7.89\pm0.12$; $83.36\pm6.53$% maximum MIP-1α response) and fluorescent intensities (log $EC_{50}=-7.84\pm0.10$; $77.34\pm5.30$% maximum MIP-1α response; $n=4$) of small endosomal vesicles containing the human CCR5-GFP receptor (Figure 10). A small antagonist-induced internalization into these small vesicles was also observed with MCP-3 (log $EC_{50}=-7.40\pm0.17$ and $-7.12\pm0.29$; $55.88\pm2.35$ and $48.70\pm2.30$% maximum MIP-1α response for N-grains and F-grains, respectively; $n=3$; Figure 10).

*Influence of aminopeptidase activity on CCR5 receptor internalization induced by met-RANTES*

It has been shown previously that incubation of met-RANTES with placental leucine aminopeptidase can cleave the N-terminal methionine and generate full agonist activity as a consequence of metabolism to the agonist RANTES (Proudfoot *et al*., 1996). Recently, an endogenous cystinyl aminopeptidase activity has been identified in CHO cell membranes with properties very similar to placental leucine aminopeptidase (Demaegdt *et al*., 2004). We, therefore, investigated whether this enzymatic activity could be responsible for the CCR5 receptor internalization induced by met-RANTES.

Incubation of CHO cells expressing the CCR5-GFP receptor with the aminopeptidase substrate L-leucine-*p*-nitroanilide in PBS demonstrated a clear linear time-dependent metabolism of the substrate to L-leucine and *p*-nitroaniline by endogenous aminopeptidases (Figure 11a). The $K_M$ for this reaction was $0.089\pm0.010$ mM ($n=6$; Figure 11b). Angiotensin IV has been shown to be a competitive inhibitor of CHO cell cystinyl aminopeptidase activity with a p$K_i$ of 6.9 (Albiston *et al*., 2003; Demaegdt *et al*., 2004). Hence, we investigated the ability of met-RANTES to induce internalization of the CCR5-GFP receptor in the presence of 1 mM angiotensin IV. However, in the presence of 1 mM angiotensin IV there was no attenuation of the ability of met-RANTES to induce internalization of CCR5-GFP

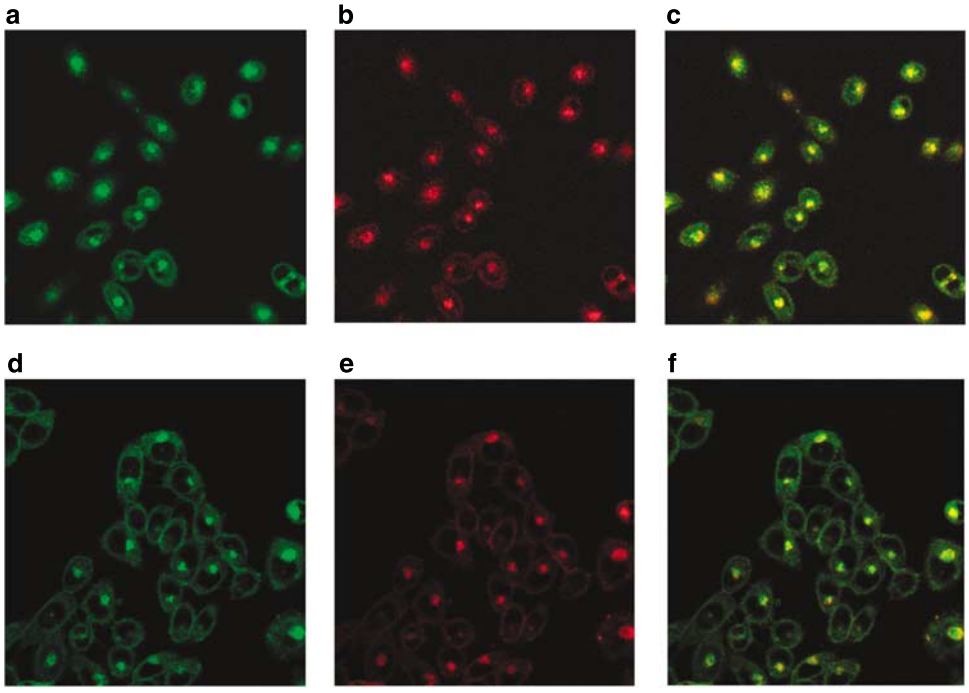


**Figure 5** Internalization of the CCR5-GFP (green fluorescent protein) receptor to the Golgi apparatus. Cells were incubated with BODIPY FL $C_5$-ceramide (5 μM; at 4 °C for 30 min) following stimulation with either macrophage inflammatory protein (MIP)-1α (CCL3, 100 nM; 37 °C, 60 min; **a**–**c**) or met-RANTES (released on activation normal T cell expressed and secreted) (1 μM; 37 °C, 60 min; **d**–**f**). The green channel (**a**, **d**) shows location of GFP and the red channel (**b**, **e**) shows the location of BODIPY TR (Texas Red). The overlays (**c**, **f**) of the two images are also shown. Confocal microscopy was performed at room temperature with the 488 nm excitation line of an argon laser with a 505–530 nm band-pass emission filter and a 560 nm long-pass emission filter. Colocalization was determined using the Zeiss LSM 510 software. Representative data are shown from three separate experiments.

receptors (Figure 11c). If anything, there was a small potentiation of the met-RANTES-induced response (Figure 11c) that may be attributable to a general protection against peptidase activity in the presence of angiotensin IV. However, 1 mM angiotensin IV only inhibited the metabolism of 0.125 mM L-leucine-*p*-nitroanilide in CHO-CCR5-GFP monolayers by 29.9 ± 1.7% ($n = 3$; Figure 11d). This indicates that there may be other active aminopeptidases present on CHO cells that can convert met-RANTES into RANTES and other active metabolites.

To gain some insight into this, we incubated CHO-CCR5-GFP cells with different concentrations of met-RANTES (0.6, 6, 60 and 600 nM) in 50 μl of HBSS for 1 h before collecting the conditioned medium; 25 μl of this medium was then applied to a second plate containing naïve CHO-CCR5-GFP cells (in 25 μl HBSS) that had been previously loaded with the calcium indicator Fluo4 (Figure 12). Under these conditions, the conditioned medium was able to stimulate a significant and rapid calcium response that was completely antagonized by 1 μM TAK 779 (Figure 12). Transfer of conditioned medium that did not contain met-RANTES was without significant effect (Figure 12). However, it was noteworthy that direct addition of 25 μl of 600 nM met-RANTES to the second plate produced no direct stimulation of calcium mobilization (Figure 12). These data suggest that there is significant metabolism of met-RANTES to an active CCR5 agonist occurring in CHO cell monolayers over a 60-min incubation period.

## Discussion

The visualization of the internalization of GPCRs by confocal microscopy (tagged with specific antibodies or fused to GFP) has led to important information on the mechanisms by which these receptors are internalized and sorted for recycling or degradation (Tarasova *et al.*, 1997; Zhang *et al.*, 1999; Conway *et al.*, 2001; Rapacciuolo *et al.*, 2003; Shenoy and Lefkowitz, 2005). However, using conventional confocal microscopy it is difficult to represent the mean response of a large population of cells in a manner that avoids the inherent bias that can be associated with the selection of appropriate fields of view. In the present study, we have used a confocal imaging plate reader to undertake an automated and quantitative analysis of the effects of CCR5 agonists and antagonists on receptor internalization in *circa* 1000 cells per well of a 96-well plate. The importance of this approach is best illustrated by reference to the example wells shown in Figures 2a and c. In response to either MIP-1α (CCL3, 100 nM) or met-RANTES (1 μM), it is clear that there are a substantial number of cells that do not respond (155 and 264 for MIP-1α and met-RANTES, respectively). This represents 13.2 and 24.7% of the total cells in each well. As a consequence, it is important to use an unbiased approach to represent the effect of each drug treatment that also takes into account the cells that do not respond.

We have investigated the effects of CCR5 ligands on the internalization of a CCR5-GFP fusion protein into either

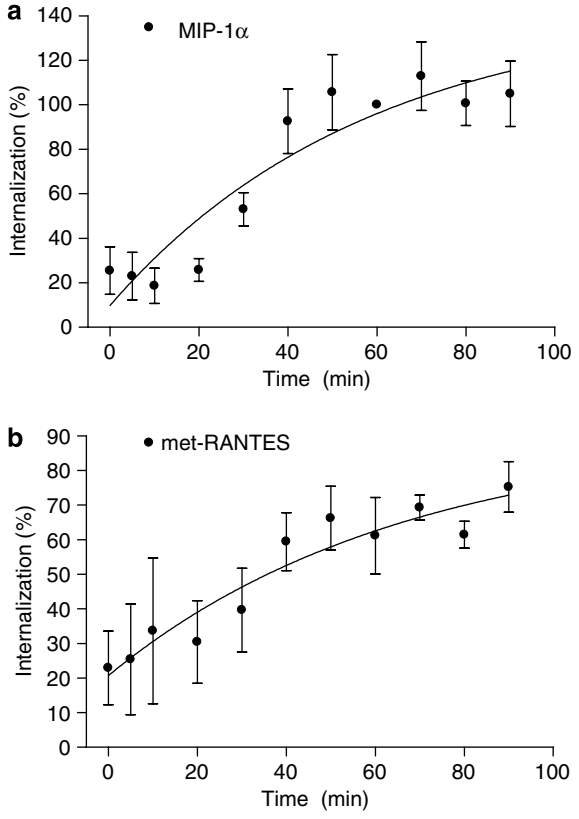


**Figure 6** Influence of macrophage inflammatory protein (MIP)-1α (CCL3) and met-RANTES (released on activation normal T cell expressed and secreted) on the internalization of the wild-type CCR5 receptor into large intracellular perinuclear focal spots. The granularity analysis algorithm of the In Cell Analyser was used to assess the fluorescence intensity (F-grains) of large grains detected using antibodies (see Materials and methods). Cells were stained with an anti-human CCR5 primary antibody (specific to the N terminus of the receptor) and then treated with chemokine before being made permeable and stained with an Alexa Fluor 633 secondary antibody to visualize the internalized receptor. The degree of antibody internalization induced at different times following cell stimulation (mean fluorescence intensity expressed as a percentage of the response to 100 nM MIP-1α at 60 min, which was measured in each experiment) in response to 100 nM MIP-1α and 1 μM met-RANTES is shown in (**a**, **b**), respectively. Values shown are mean ± s.e.mean from six (MIP-1α, **a**) and three (met-RANTES, **b**) separate experiments.

large perinuclear focal spots (which appear to represent the Golgi apparatus based on colocalization with BODIPY FL $C_5$-ceramide) or small endosomal vesicles (Lim *et al*., 2001). In general, only one large perinuclear grain was detected within a given cell (although occasionally two were present). We assessed the mean fluorescence intensities per cell in these perinuclear focal spots or endosomal vesicles and the total number of endosomal vesicles, in response to different CCR5 ligands. As expected, the CCR5 agonists MIP-1α (CCL3), MIP-1β (CCL4) and RANTES (CCL5) stimulated a substantial internalization of the CCR5-GFP receptor. The response was rapid, with an increase in both the number and average fluorescence intensities of endosomal vesicles, reaching a maximum between 20 and 40 min with MIP-1α. The increase in fluorescence intensity of the larger perinuclear spots was a slower process, reaching a maximum by *circa* 60 min. Experiments undertaken with filipin and intracellular acidification with acetic acid (pH 5) strongly suggest that agonist-stimulated internalization of the CCR5 receptor is via clathrin-coated pits (Sandvig *et al*., 1987; Orlandi and Fishman, 1998). This is consistent with results from studies using the $\beta_2$-adrenoceptor and suggests that GPCRs are phosphorylated by GPCR kinases in response to agonists. This in turn leads to the recruitment of β-arrestins and subsequent targeting of the GPCR for internalization via clathrin-coated pits (Ferguson *et al*., 1998; Luttrell and Lefkowitz, 2002; Marchese *et al*., 2003). Chemokine receptor agonists have been shown previously to phosphorylate the CCR5 receptor on four C-terminal serine residues as a consequence of both GPCR kinase and protein kinase C activation (Oppermann *et al*., 1999). Furthermore, β-arrestin has been shown to interact with some of these C-terminal phosphorylation sites of the CCR5 receptor (Huttenrauch *et al*., 2002).

The response to MIP-1α was potently antagonized by the non-peptide CCR5 antagonist TAK 779. However, when the peptide-based CCR5 antagonists were studied the results were rather surprising. All four of those evaluated were able to inhibit potently MIP-1α-mediated increases in calcium mobilization. However, eotaxin-3 (CCL26) and MCP-3 (CCL7) (both at 1 μM) had very little effect on the MIP-1α concentration–response curve for CCR5-GFP receptor internalization (data not shown). vMIP-II produced only a small antagonism of the MIP-1α response, whereas met-RANTES appeared to augment the response to MIP-1α. Closer evaluation of the effect of met-RANTES showed that it directly stimulated CCR5-GFP receptor internalization in a manner that was completely sensitive to inhibition by the non-peptide CCR5 antagonist TAK 799 (Baba *et al*., 1999).

Met-RANTES was also able to stimulate internalization of the wild-type CCR5 receptor, suggesting that the C-terminal GFP tag does not influence this activity. met-RANTES stimulated an increase in both the number and fluorescence intensities of small endosomal vesicles in CHO cells expressing the CCR5-GFP receptor. Interestingly, there was also a small stimulating effect of MCP-3 on internalization to endosomal vesicles. The mechanisms utilized by these antagonists appeared to be very similar to the agonist chemokines as the response was insensitive to filipin, but could be completely inhibited by cytosolic acidification. This suggests that a β-arrestin-clathrin-coated pit mechanism is involved. It is well established that compounds such as met-RANTES are antagonists of CCR5 and are not able to stimulate chemotaxis (Proudfoot *et al*., 1996). We have also provided evidence that met-RANTES is able to inhibit MIP-1α-mediated calcium responses without producing a direct effect on calcium itself. This raises the question of how the recruitment of the CCR5 receptor to clathrin-coated pits and receptor internalization can be achieved following met-RANTES stimulation.

There is some evidence that stimulation of interactions between GPCRs and arrestins can occur in response to specific antagonists (Gray and Roth, 2001). There is also increasing evidence that the nature of the receptor–arrestin interaction may not be entirely dependent upon agonist-stimulated receptor phosphorylation. For example, Azzi *et al*.

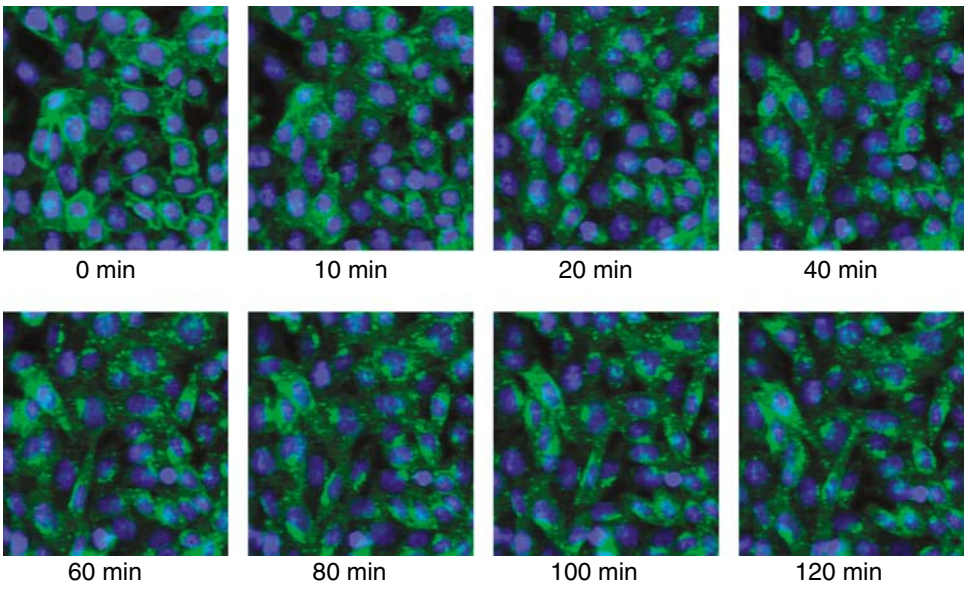


**Figure 7** Internalization of CCR5-GFP (green fluorescent protein) induced by met-RANTES (released on activation normal T cell expressed and secreted) in live cells. Representative images are shown from one well of cells stimulated with 600 nM met-RANTES and imaged live on the IN Cell analyser 3000. Cells were stained with Hoechst 33342 and treated with met-RANTES (as described in Materials and methods) before being immediately transferred to the IN Cell Analyser 3000 and imaged every 10 min for 120 min at 37 °C, 5% $CO_2$ and 75% humidity.

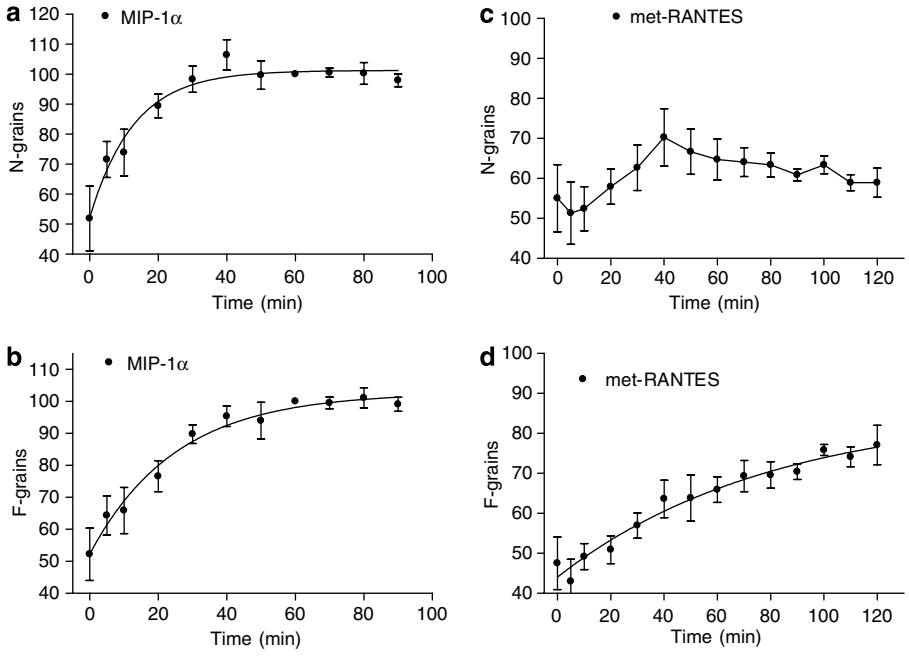


**Figure 8** Time course of macrophage inflammatory protein (MIP)-1α- (CCL3) and met-RANTES (released on activation normal T cell expressed and secreted)-stimulated internalization of CCR5-GFP (green fluorescent protein) receptors into endosomal small vesicles. The granularity algorithm of the In Cell Analyser was used to assess both the number (N-grains) and the fluorescence intensity (F-grains) of small grains as described in Materials and methods. The degree of CCR5-GFP internalization at different times of stimulation (mean fluorescence intensity or grain number expressed as a percentage of the response to 100 nM MIP-1α at 60 min, which was measured in each experiment) in response to 100 nM MIP-1α (**a**, **b**) and 1 μM met-RANTES (**c**, **d**) is shown for both N-grains (**a**, **c**) and F-grains (**b**, **d**). Values (mean ± s.e.mean) are from three (basal, **b**), six (MIP-1α, **b**) and six (met-RANTES, **d**) separate experiments. Please not that the ordinates in all four panels do not begin at zero.

have recently demonstrated that certain β-adrenoceptor inverse agonists can stimulate MAP kinase activation in a β-arrestin-dependent manner in HEK 293 cells overexpressing the $\beta_2$-adrenoceptor. It has also been shown, by surface plasmon resonance, that purified β-arrestin-1 can bind to both phosphorylated and non-phosphorylated CCR5 C-terminal tail peptides with equal affinity (Huttenrauch *et al*., 2002). Finally, a number of receptor antagonists have also been found to stimulate internalization of 5-$HT_{2A}$ and cholecystokinin type A receptors in the absence of any

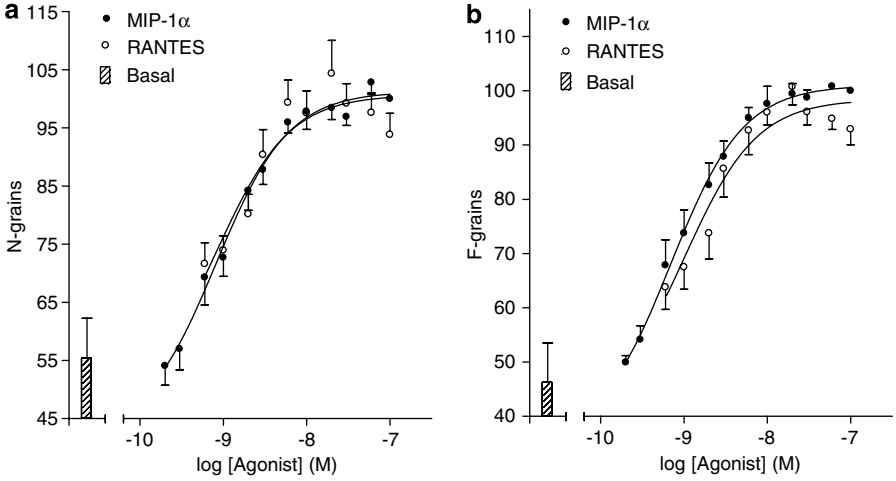


**Figure 9** Concentration–response curves for macrophage inflammatory protein (MIP)-1α- (CCL3) and RANTES (released on activation normal T cell expressed and secreted)-stimulated internalization of CCR5-GFP (green fluorescent protein) receptors into endosomal small vesicles. The granularity algorithm of the In Cell Analyser was used to assess both the number (**a**; N-grains) and the fluorescence intensity (**b**; F-grains) of small grains as described in Materials and methods. Mean fluorescence intensity or grain number values are expressed as a percentage of the response to 100 nM MIP-1α at 60 min, which was measured in each experiment. Values are mean ± s.e.mean from 10 (MIP-1α) and 9 (RANTES) separate experiments. Please note that the ordinates do not begin at zero.

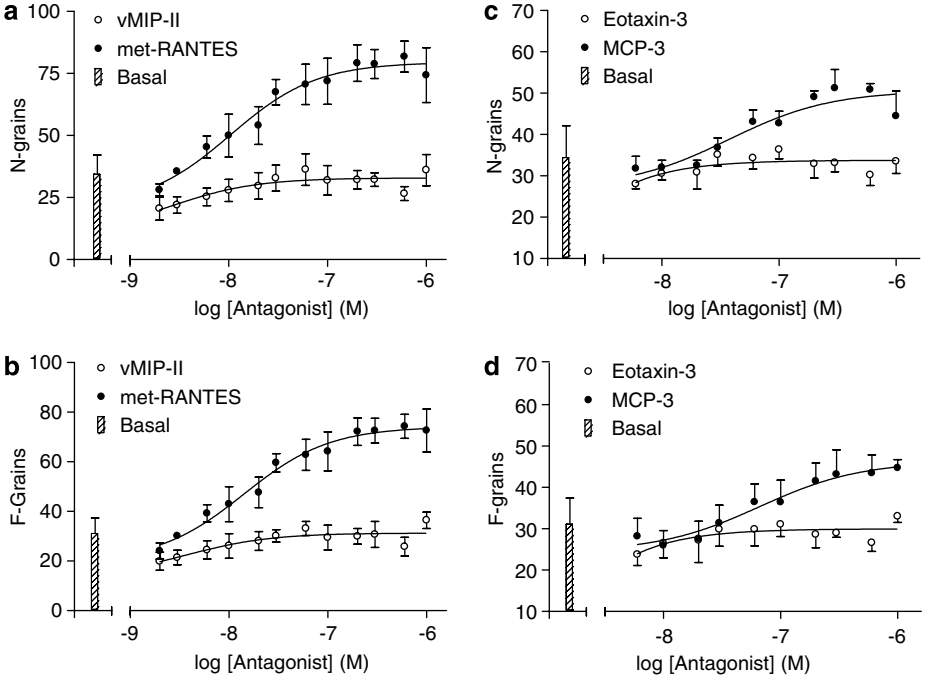


**Figure 10** Concentration–response curves for met-RANTES (released on activation normal T cell expressed and secreted)-, vMIP-II-, eotoxin-3- (CCL26) and MCP-3 (CCL7)-stimulated internalization of CCR5-GFP (green fluorescent protein) receptors into endosomal small vesicles. The granularity algorithm of the In Cell Analyser was used to assess both the number (**a**, **c**; N-grains) and fluorescence intensity (**b**, **d**; F-grains) of small grains as described in Materials and methods. Mean fluorescence intensity or grain number values are expressed as a percentage of the response to 100 nM MIP-1α at 60 min, which was measured in each experiment. Values are mean ± s.e.mean from three (four for met-RANTES) separate experiments. Please note that in (**c**, **d**) the ordinate does not begin at zero.

measurable agonist activity (Roettger *et al*., 1997; Gray and Roth, 2001).

It has been previously shown that incubation of met-RANTES with placental leucine aminopeptidase can cleave the N-terminal methionine and generate full agonist activity as a consequence of metabolism to the agonist RANTES (Proudfoot *et al*., 1996). It is therefore possible that met-RANTES may induce CCR5 receptor internalization as a consequence of a conversion to RANTES or other active metabolite. Recently, an endogenous cystinyl aminopeptidase activity has been identified in CHO cell membranes with properties very similar to placental leucine aminopeptidase (Demaegdt *et al*., 2004). This enzyme is also called insulin-regulated membrane aminopeptidase and it has

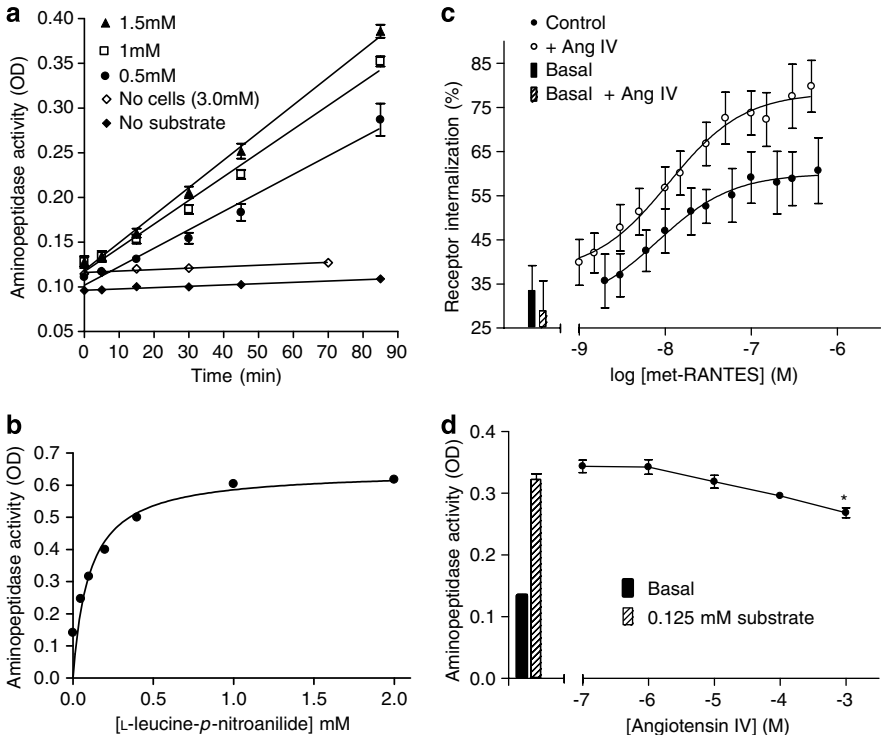


**Figure 11** Influence of the cystinyl aminopeptidase inhibitor angiotensin IV (1 mM; Ang IV) on aminopeptidase activity in Chinese hamster ovary (CHO)-CCR5-GFP (green fluorescent protein) cells and CCR5 receptor internalization. (**a**) Aminopeptidase activity in monolayers of CHO-CCR5-GFP cells. Cells were incubated with different concentrations of the substrate L-leucine-*p*-nitroanilide in 200 μl phosphate-buffered saline (PBS) at 37 °C and the production of *p*-nitroaniline was monitored as the optical density (OD) at 405 nm. In addition, the metabolism of 3 mM substrate over time in 200 μl of PBS was monitored in the absence of cells. Values are mean ± s.e.mean of six replicates in a single experiment, which is representative of four separate experiments. (**b**) Representative experiment showing the concentration–response relationship for the metabolism of L-leucine-*p*-nitroanilide in CHO-CCR5-GFP cells incubated in 100 μl of PBS for 60 min. Values are mean ± s.e.mean of six replicates in a single experiment, which is representative of six separate experiments. (**c**) Influence of the cystinyl aminopeptidase inhibitor angiotensin IV (1 mM; Ang IV) on met-RANTES (released on activation normal T cell expressed and secreted)-induced CCR5-GFP internalization into large perinuclear grains. Values shown are mean ± s.e.mean from five (met-RANTES alone) and five (met-RANTES + Ang IV) separate experiments. (**d**) Inhibition by angiotensin IV of the metabolism of 0.125 mM L-leucine-*p*-nitroanilide in CHO-CCR5-GFP cells incubated in 100 μl of PBS for 60 min. Values are mean ± s.e.mean of six replicates in a single experiment, which is representative of three separate experiments. *$P<0.01$ versus substrate alone (one-way ANOVA). Please note that in (**a**, **c**) the ordinate does not begin at zero.

recently been shown to be the so-called angiotensin IV receptor (Albiston *et al*., 2003). Angiotensin IV is a potent inhibitor of this aminopeptidase catalytic activity (Lew *et al*., 2003) and can competitively inhibit CHO cell cystinyl aminopeptidase activity (p$K_i$ of 6.9; Demaegdt *et al*., 2004). In the present study, inclusion of 1 mM angiotensin IV did not attenuate the ability of met-RANTES to stimulate CCR5-GFP receptor internalization. Rather, the response to met-RANTES was enhanced. It is therefore unlikely that conversion of met-RANTES into RANTES via an angiotensin IV-sensitive aminopeptidase enzyme is responsible for the stimulation of receptor internalization. However, it was noteworthy that an aminopeptidase activity could be detected in monolayers of CHO-CCR5-GFP cells that were relatively resistant to angiotensin IV. Furthermore, incubation of CHO-CCR5-GFP or native CHO cells with met-RANTES (0.6–600 nM) for 60 min released sufficient CCR5 agonist activity (as determined by its sensitivity to inhibition by TAK 779) into the medium to be able to activate a rapid calcium response in naïve CHO-CCR5-GFP cells, despite the continued presence of any non-metabolized met-RANTES in the medium. These data strongly suggest that there is an endogenous aminopeptidase activity on the surface of CHO cells that can produce a slow internalization of the receptor following a time-dependent conversion of met-RANTES from a CCR5 receptor antagonist into a CCR5 agonist molecule. An intriguing question is whether this occurs while met-RANTES is bound to the CCR5 receptor? In many ways this is the most likely scenario, given that met-RANTES has high affinity (*circa* 10 nM) for CCR5 (Proudfoot *et al*., 1996) and will bind, initially in its un-metabolized form, with high occupancy to CCR5 in the concentration range used to stimulate significant receptor internalization (10–100 nM). Given that the dissociation of chemokines from the receptor is generally slow (Springael *et al*., 2006), it is difficult to envisage that the generation of agonist-like metabolites in the bulk phase of the extracellular fluid will be sufficient to replace already receptor-bound met-RANTES to the extent required to stimulate CCR5 internalization. CCR5 internalization induced by met-RANTES was observed with an $EC_{50}$ of 10–30 nM. However, it was noteworthy that a significant change in intracellular $Ca^{2+}$ following preincubation with CHO cells for 60 min and then transfer to naïve CHO-CCR5-GFP cells was only observed with 300 nM met-RANTES (Figure 12). In this latter situation, it is also worth emphasizing that un-metabolized met-RANTES and agonist

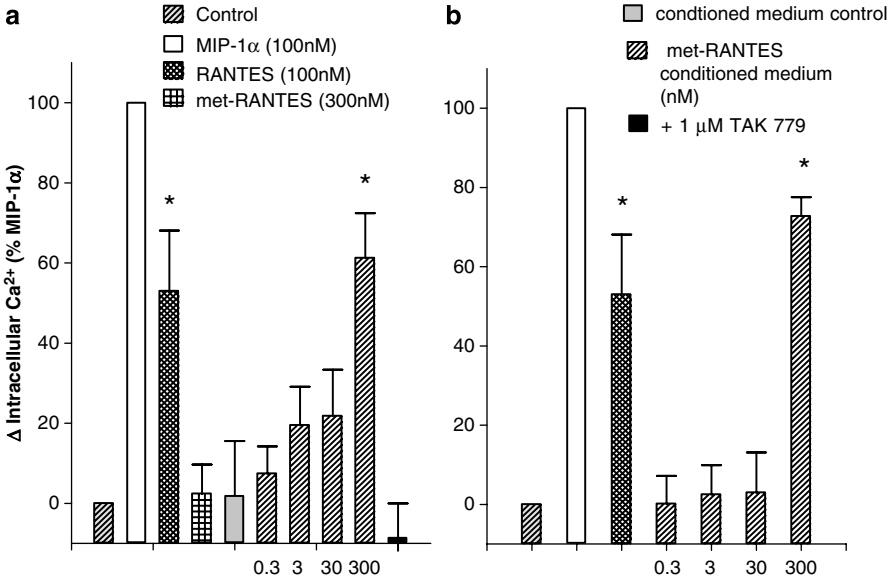


**Figure 12** Metabolism of met-RANTES (released on activation normal T cell expressed and secreted) to a calcium-mobilizing species in (**a**) CHO-CCR5-GFP (green fluorescent protein) cells or (**b**) CHO (Chinese hamster ovary) cells. A donor 96-well plate containing (**a**) CHO-CCR5-GFP cells or (**b**) CHO cells was incubated with Hank's balanced salt solution (HBSS) or HBSS containing 0.6, 6, 60 and 600 nM met-RANTES, in a total volume of 50 μl for 60 min. The conditioned medium was collected and then a 25 μl sample of each was added to a second (acceptor) 96-well plate of CHO-CCR5-GFP cells (**a**, **b**) incubated in 25 μl HBSS that had been pre-loaded with Fluo4. Concentrations of met-RANTES on the *X*-axis indicate final theoretical concentrations of met-RANTES in the acceptor plate. Samples, 25 μl, of HBSS (control), 200 nM MIP-1α (CCL3), 200 nM RANTES (CCL5) and 600 nM met-RANTES were also added directly to the donor plate. Finally, 25 μl of the conditioned medium following exposure of the donor plate to 600 nM met-RANTES for 60 min was added to wells of the acceptor plate that had been pre-incubated with 1 μM TAK 779. Intracellular levels of calcium were monitored in the acceptor plate using a fluorometric imaging plate reader (FLIPR3) as described in Materials and methods. Values are expressed as a percentage of the maximum response to 100 nM MIP-1α and represent mean ± s.e.mean of four separate experiments, which were each conducted with eight replicate determinations of each condition. $^*P<0.01$ versus basal (one-way ANOVA).

metabolite were delivered simultaneously to naïve CHO-CCR5-GFP on transfer of the conditioned medium.

These observations have important implications for the use of met-RANTES as an antagonist of CCR5-mediated responses. The secondary 'antagonist' effect produced by met-RANTES, as a consequence of aminopeptidase activity and agonist metabolite-stimulated receptor internalization, may represent a novel mechanism by which receptors can be removed from the cell surface without producing a coordinated agonist response throughout the cell. This combination of CCR5 receptor antagonism and slow metabolite-induced receptor endocytosis may also provide a useful mechanism for limiting the availability of cell surface CCR5 receptors for interaction with the viral envelope proteins of HIV.

## Acknowledgements

We thank AstraZeneca Research and Development for financial support.

## Conflict of interest

SJH (none). JL was a PhD student supported by AstraZeneca. EC is employed by AstraZeneca.

## References

Albiston AL, Mustafa T, McDowall SG, Mendelsohn AO, Lee J, Chai SY (2003). AT4 receptor is insulin-regulated membrane aminopeptidase: potential mechanisms of memory enhancement. *Trends Endocrinol Metab* **14**: 72–77.

Azzi M, Charest PG, Angers S, Rousseau G, Kohout T, Bouvier M *et al.* (2003). Beta-arrestin-mediated activation of MAPK by inverse agonists reveals distinct active conformations for G protein-coupled receptors. *Proc Natl Acad Sci USA* **100**: 11406–11411.

Baba M, Nishimura O, Kanzaki N, Okamato M, Sawada H, Iizawa Y *et al.* (1999). A small molecule, nonpetide, CCR5 antagonist with highly potent and selective anti-HIV-1 activity. *Proc Natl Acad Sci USA* **96**: 5698–5703.

Barak LS, Ferguson SSG, Zhang J, Caron MG (1997). A beta-arrestin-green fluorescent protein biosensor for detecting G protein-coupled receptor activation. *J Biol Chem* **272**: 27497–27500.

Carman CV, Benovic JL (1998). G-protein-coupled receptors: turn-ons and turn-offs. *Curr Opin Neurobiol* **8**: 335–344.

Conway BR, Minor LK, Xu JZ, D'Andrea MR, Ghosh RN, Demarest KT (2001). Quantitative analysis of agonist-dependent parathyroid hormone receptor trafficking in whole cells using a functional green fluorescent protein conjugate. *J Cell Physiol* **189**: 341–355.

Demaegdt H, Vanderheyden P, De Baker JP, Mosselmans S, Laeremans H, Le MT *et al.* (2004). Endogenous cystinyl aminopeptidase in Chinese hamster ovary cells: characterization by [$^{125}$I] Ang IV binding and catalytic activity. *Biochem Pharmacol* **68**: 885–892.

Ferguson SSG, Zhang J, Barak LS, Caron MG (1998). Molecular mechanisms of G protein-coupled receptor desensitization and resensitization. *Life Sci* **62**: 1561–1565.

Gray JA, Roth BL (2001). Paradoxical trafficking and regulation of 5-HT$_{2A}$ receptors by agonists and antagonists. *Brain Res Bull* **56**: 441–451.

Heuser JE, Anderson RG (1989). Hypertonic media inhibit receptor-mediated endocytosis by blocking clathrin-coated pit formation. *J Cell Biol* **108**: 389–400.

Huttenrauch F, Nitki A, Lin F-J, Honing S, Oppermann M (2002). Arrestin binding to CC chemokine receptor 5 requires multiple C-terminal receptor phosphorylation sites and involves a conserved Asp-Arg-Tyr sequence motif. *J Biol Chem* **277**: 30769–30777.

Johnson Z, Schwartz M, Power CA, Wells TNC, Proudfoot AEI (2005). Multi-faceted strategies to combat disease by interference with the chemokine system. *Trends Immunol* **26**: 268–274.

Kahout TA, Lefkowitz RJ (2003). Regulation of G-protein-coupled receptor kinases and arrestins during receptor desensitization. *Mol Pharmacol* **63**: 9–18.

Kazmierski W, Bifulco N, Yang H, Boone L, DeAnda F, Watson C *et al*. (2003). Recent progress in discovery of small molecule CCR5 chemokine receptor ligands as HIV-1 inhibitors. *Bioorg Med Chem* **11**: 2663–2676.

Lew RA, Mustafa T, Ye S, McDowell SG, Chai SY, Albiston AL (2003). Angiotensin $AT_4$ ligands are potent, competitive inhibitors of insulin regulated aminopeptidase (IRAP). *J Neurochem* **86**: 344–350.

Lim S-N, Bonzelius F, Low SH, Wille H, Weimbs T, Herman GA (2001). Identification of discrete classes of endosome-derived small vesicles as a major cellular pool for recycling membrane proteins. *Mol Biol Cell* **12**: 981–995.

Luttrell LM, Lefkowitz RJ (2002). The role of β-arrestins in the termination and transduction of G-protein-coupled receptor signals. *J Cell Sci* **115**: 455–465.

Luttrell LM, Roudabush FL, Choy EW, Miller WE, Field ME, Pierce KL *et al*. (2001). Activation and targeting of extracellular-signal-regulated kinases by β-arrestin scaffolds. *Proc Natl Acad Sci USA* **98**: 2449–2454.

Mack M, Luckow B, Nelson PJ, Cihak J, Simmons G, Clapham PR *et al*. (1998). Aminooxypentane-RANTES induces CCR5 internalization but inhibits recycling: a novel inhibitory mechanism of HIV infectivity. *J Exp Med* **187**: 1215–1224.

Marchese A, Chen C, Kim Y-M, Benovic JL (2003). The ins and outs of G-protein-coupled receptor trafficking. *Trends Biochem Sci* **28**: 369–376.

Oppermann M, Mack M, Proudfoot AE, Olbrich H (1999). Differential effects of CC chemokines on CC chemokine receptor 5 (CCR5) phosphorylation and identification of phosphorylation sites on the CCR5 carboxyl terminus. *J Biol Chem* **274**: 8875–8885.

Orlandi PA, Fishman PH (1998). Filipin-dependent inhibition of cholera toxin: evidence for toxin internalization and activation through caveolae-like domains. *J Cell Biol* **141**: 905–915.

Proudfoot AEI, Power CA, Hoogewerf AJ, Montjovent M-O, Borlat F, Offord RE *et al*. (1996). Extension of recombinant human RANTES by the retention of the initiating methionine produces a potent antagonist. *J Biol Chem* **271**: 2599–2603.

Rapacciuolo A, Suvarna S, Barki-Harrington L, Luttrell LM, Cong M, Lefkowitz RJ *et al*. (2003). Protein kinase A and G protein-coupled receptor kinase phosphorylation mediates β-1 adrenergic receptor endocytosis through different pathways. *J Biol Chem* **278**: 35403–35411.

Roettger BF, Ghanekar D, Roa R, Toledo C, Yingling J, Pinon D *et al*. (1997). Antagonist-stimulated internalization of the G protein-coupled cholecystokinin receptor. *Mol Pharmacol* **51**: 357–362.

Rot A, Von Andrian UH (2004). Chemokines in innate and adaptive host defence: basic chemokinese grammar for immune cells. *Ann Rev Immunol* **22**: 891–928.

Sandvig K, Olsnes S, Petersen OW, Van Deurs B (1987). Acidification of the cytosol inhibits endocytosis from coated pits. *J Cell Biol* **105**: 679–689.

Seta K, Nanamori M, Modrall JG, Neubig RR, Sadoshima J (2002). AT1 receptor mutant lacking heterotrimeric G protein coupling activates the Src-Ras-ERK pathway without nuclear translocation of ERKs. *J Biol Chem* **277**: 9268–9277.

Shenoy SK, Lefkowitz RJ (2005). Receptor-specific ubiquitination of β-arrestin directs assembly and targeting of seven-transmembrane receptor signalosomes. *J Biol Chem* **280**: 15315–15324.

Signoret N, Pelchen-Matthews A, Mack M, Proudfoot AEI, Marsh M (2000). Endocytosis and recycling of the HIV coreceptor CCR5. *J Cell Biol* **151**: 1218–1293.

Simmons G, Reeves JD, Hibbitts S, Stine JT, Gray PW, Proudfoot AEI *et al*. (2000). Co-receptor use by HIV and inhibition of HIV infection by chemokine receptor ligands. *Immunol Rev* **177**: 112–126.

Springael JY, Minh PML, Urizar E, Costagliola S, Vassart G, Parmentier M (2006). Allosteric modulation of binding properties between units of chemokine receptor homo- and hetero-oligomers. *Mol Pharmacol* **69**: 1652–1661.

Tarasova NI, Stauber RH, Choi JK, Hudson EA, Czerwinski G, Miller JL *et al*. (1997). Visualization of G-protein-coupled receptor trafficking with the aid of green fluorescent protein. *J Biol Chem* **272**: 14817–14824.

Terrillon S, Bouvier M (2004). Receptor activity-independent recruitment of βarrestin2 reveals specific signalling modes. *EMBO J* **23**: 3950–3961.

Tohgo A, Pierce KL, Choy EW, Lefkowitz RJ, Luttrell LM (2002). β-Arrestin scaffolding of the ERK cascade enhances cytosolic ERK activity but inhibits ERK-mediated transcription following angiotensin AT1a receptor stimulation. *J Biol Chem* **277**: 9429–9436.

Wei H, Ahn S, Shenoy SK, Karnik SS, Hunyadi L, Luttrell LM *et al*. (2003). Independent β-arrestin2 and G-protein-mediated pathways for angiotensin II activation of extracellular signal regulated kinases 1 and 2. *Proc Natl Acad Sci USA* **100**: 10782–10787.

Zhang J, Barak LS, Anborgh PH, Laporte SA, Caron MG, Ferguson SSG (1999). Cellular trafficking of G protein-coupled receptor/β-arrestin endocytic complexes. *J Biol Chem* **274**: 10999–11006.